SECTORAL M-EBG ANTENNA WITH MULTIPOLARIZATION CAPABILITIES FOR WIMAX BASE STATIONS

M. Hajj[1, *], R. Chantalat[1], M. Lalande[2], and B. Jecko[2]

[1]CISTEME
Ester Technopole, Limoges 87069, France

[2]Faculté des Sciences et Techniques, XLIM, CNRS UMR 6172
123 Avenue Albert Thomas, Limoges 87060, France

Abstract—A novel multipolarized sectoral antenna on a metallic electromagnetic band gap (M-EBG) surface is investigated. The M-EBG structure behaves as a partially reflecting surface (PRS) and enhances the directivity of a simple radiating source. The use of metallic structures offers a new approach to industrial partners in order to reduce costs and to facilitate design techniques. By using double layers of M-EBG structure working on orthogonal polarizations as a superstrate with a single patch feeding by two ports, multipolarization operation is achieved. This antenna provides vertical, horizontal, $0°/90°$ and circular polarizations with a sectoral radiation pattern in the azimuth plane. M-EBG antennas with sectoral pattern are usually designed only for vertical polarization. In order to verify the results a Bipolar M-EBG Sectoral antenna prototype for WIMAX application [5.15–5.35] GHz is realized and measured. Finally, we study the possibility to generate circular polarization.

1. INTRODUCTION

The demand for higher capacity on wireless communication system led to the development of multipolarized antenna. Furthermore, an antenna which generates a sectoral pattern with equal horizontal and vertical components will provide higher diversity gain [1] in all directions.

The sectoral antenna is ideal for mobile applications. These Base Station antennas also provide a large side lobe for providing coverage right underneath the antenna when mounted on a mast. The multipolarized nature makes them the ideal partner in highly reflective environments where one can never be certain of the polarization of the received signal.

For the last years, the requests for multipolarized antennas have increased. They are used in many applications such as radars and satellite communication systems. Indeed, these antennas are used when the orientation of a linearly polarized signal cannot be predicted. These systems must present the same characteristics as an antenna with linear polarization (high gain, simplicity of realization, etc.).

Horizontal and vertical polarized antennas are adopted at first because it is easy to realize, but the efficiency of the vertical polarized antenna used in wireless communication base station is higher than that of the horizontal polarized antenna. Recently, people choose multipolarized antenna. Microstrip dual-polarized antenna is popular [2–4]. People usually adopt microstrip antenna to realize the dual polarization but this type of antenna array requires complicated structures of distribution circuits.

M-EBG antennas have attracted considerable interest in recent years due to their advantages of high directivity, low sidelobe, simple structure and relatively low-profile [5–9].

Typically, these antennas consist of a M-EBG structure, such as a frequency selective surface (FSS) or partially reflective surface (PRS), placed approximately half a wavelength above a ground plane containing a source antenna [10–12].

An example of a directive M-EBG antenna is given on Fig. 1, where the M-EBG structure is constituted by a layer of square metallic rods.

According to this method, a new concept of sectoral M-EBG antenna working in vertical linear polarization was developed in our laboratory [13]. It is interesting to examine the various options to realize a multipolarized sectoral M-EBG antenna.

In this paper, we use double M-EBG layers with orthogonal polarizations and corporate excitation patch fed by two probes to design the multipolarized sectoral antenna. A 0°/90° dual polarized M-EBG sectoral antenna was designed at first in order to obtain equal vertical and horizontal electric field components. A realization and its measurement results are then proposed. The circular polarization with improvement technique is presented in the third part.
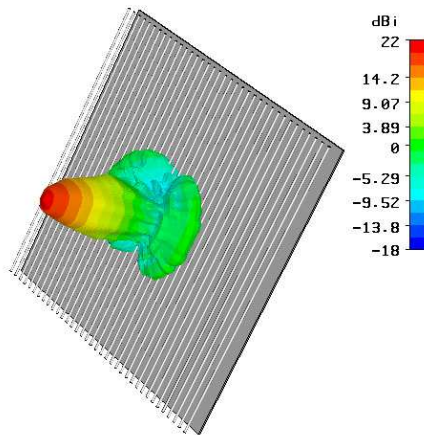
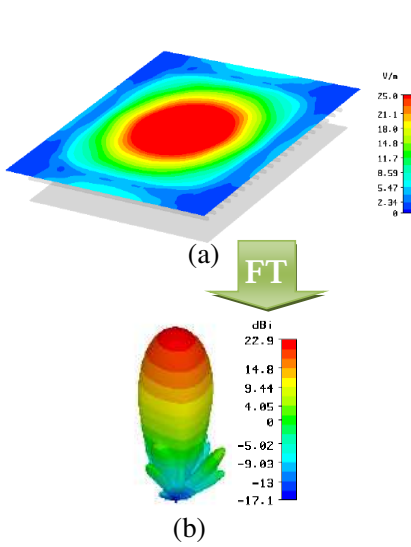**Figure 1.** Example of directive M-EBG antenna.

2. PRINCIPLE OF SECTORAL M-EBG ANTENNA

The radiation pattern of an M-EBG antenna being created by a radiating aperture, one only need to modify the latter's properties and shape to obtain the desired form. This is due to the fact that the radiation pattern is the Fourier transform of the spot at the antenna aperture.

The radiant aperture of a square directive M-EBG antenna (Fig. 1) has a circular form, as illustrated in Fig. 2(a). Therefore, the radiation pattern presents the same aperture in both vertical and horizontal planes (Fig. 2(b)) [5–8].

The sectoral radiation pattern design (Fig. 3(a)) can be inspired from directive M-EBG antennas by transforming the circular radiant aperture to an elliptical one, as shown in (Fig. 3(b)). This can be achieved with a M-EBG antenna, provided that the energy propagation is impaired in one direction of the azimuth plane. This transformation is done by giving the M-EBG structure a rectangular form. The use of vertical PEC (Fig. 4) to limit the energy propagation along the horizontal plane results in the desired effect, thus creating the sought after radiation pattern.

The functioning of such a structure is quite similar to a classic rectangular waveguide working on the TE01 mode, except for the energy transmitted through the M-EBG material. The working frequency of the antenna can thus be obtained through the following

Figure 2. (a) Circular aperture, (b) 3D radiation pattern of a square directive MEBG antenna.
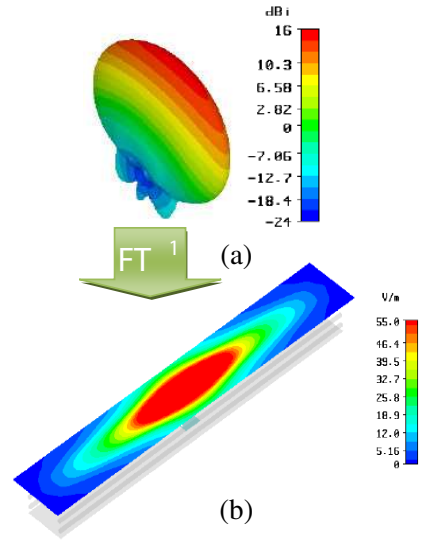
Figure 3. (a) 3D radiation pattern of a rectangular sectoral M-EBG antenna, (b) elliptical aperture.
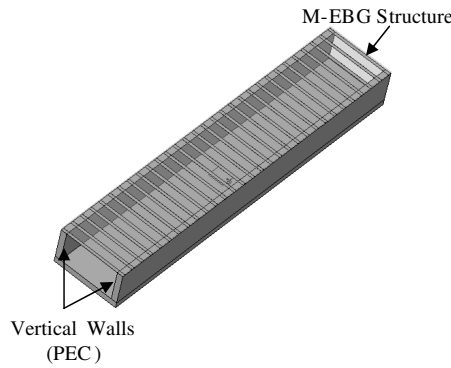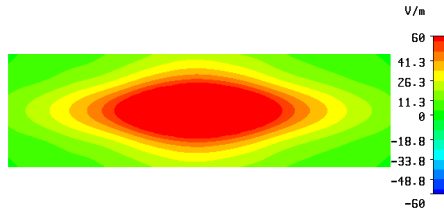

Figure 4. Sectoral M-EBG antenna structure.

relation [9, 14].

$$f = \frac{c}{2h}\left(\frac{1}{2} + \frac{\varphi_{M-EBG}}{2\pi}\right) \tag{1}$$

With h the antenna height, φ_{M-EBG} corresponds to the reflection phase of the M-EBG structure.

Figure 5. Field distribution inside the sectoral M-EBG antenna.

Due to the waveguide-like comportment of the antenna, the E field on the radiating aperture shows no variation along the transverse axis (Fig. 5). Along the antenna's length, an exponential attenuation can be observed as the antenna works under the guide cutoff frequency.

The radiation angle can therefore be approximated through the relation below, according to the general theory on rectangular radiating aperture [15].

$$\theta_{-3\,\mathrm{dB}} = \frac{50.8 * \lambda}{l} \qquad (2)$$

where θ is the beamwidth in the azimuth plane, and l is the antenna width.

The design of the M-EBG structure will then determine the antenna maximum directivity and operating bandwidth, as in the case of more classic directive EBG structures [5–11]. Furthermore, the potential directivity and the half power bandwidth are functions of the resonator quality factor Q for a M-EBG antenna. Moreover, the quality factor Q depends on the reflection coefficient of the M-EBG material $|r_{M-EBG}|e^{j\varphi M-EBG}$ at the operating frequency f_0, as proven in the Equation (3), [14].

$$Q(f_0) = \frac{\sqrt{|r_{M-EBG}(f_0)|}}{1 - |r_{M-EBG}(f_0)|} \left(\frac{1}{2} + \frac{\varphi_{M-EBG}(f_0)}{2\pi} \right) \qquad (3)$$

3. HORIZONTALLY POLARIZED SECTORAL M-EBG ANTENNA

The objective is to design an antenna still intended for wireless telecommunication networks base stations. Our sectoral M-EBG antenna must satisfy the WIMAX specifications [5.15–5.35] GHz with 15 dB directivity and a radiation beamwidth of at least $60°$ in the horizontal plane. This antenna uses only unidimensionnal metallic structures working in TM polarization: feed ports and metallic rods
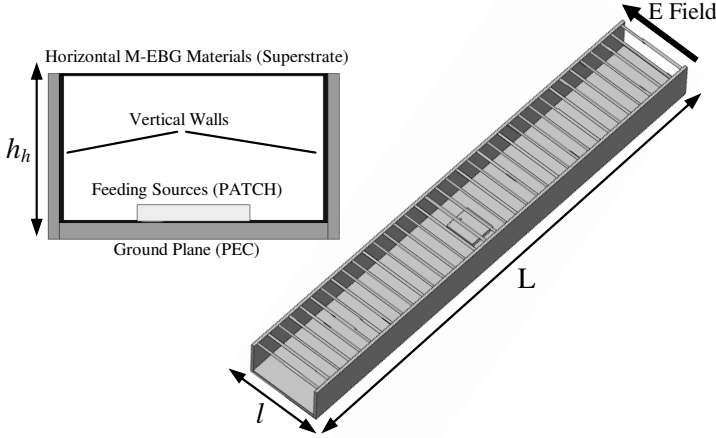
Figure 6. Top and 3D view of the horizontally polarized sectoral M-EBG antenna.

must be in a horizontal distribution. To reduce the antenna cost, we choose a M-EBG structure composed by simple rods.

The proposed antenna configuration is shown in Fig. 6. It is composed of three principal parts:

1. The ground plane where the feeding system (simple patch) is located.
2. The cavity located between the ground plane and the M-EBG layer.
3. The M-EBG structure made by periodic metallic elements.

The working frequency depends on the reflection coefficient of the M-EBG material. To calculate the phase, we have used the frequency domain solver of CST Microwave Studio.

This solver allows simulating a unit cell of the M-EBG structure, by defining periodic boundaries at its beginning and its end [16].

The height of the resonant cavity can be obtained through the following relation (4) [9, 14]:

$$h_h = \frac{\lambda}{2}\left(\frac{1}{2} + \frac{\varphi_{M-EBG}}{2\pi}\right) \tag{4}$$

With $\varphi_{M-EBG} = 157.5°$ at 5.3 GHz correspond to the reflection phase of the M-EBG structure.

According to the antenna description, its width will directly determine the radiation angle which has to meet the 60° requirement.

The application of the formula given in the previous paragraph yields a value of $l = 52$ mm, calculated at the upper limit of the frequency band intended for the antenna.

With the antenna width calculated above, 15 dB directivity requires a $L = 375$ mm length for a rectangular aperture with a uniform field distribution. The M-EBG layer will then be designed to ensure such a length for the radiating aperture.

The horizontal M-EBG layer is composed of 36 metallic rods of 52×2 m^2 and 10.5 mm periodicity.

The simulated ground plane has the same size as the structure, i.e., $L = 375$ mm $\times l = 52$ mm.

The feeding system is created by one patch placed at the center of the cavity above the ground plane.

The simulated directivity vs. frequency is shown on Fig. 7.
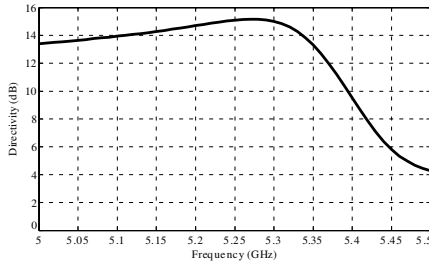
Figure 7. Directivity evolution versus frequency.
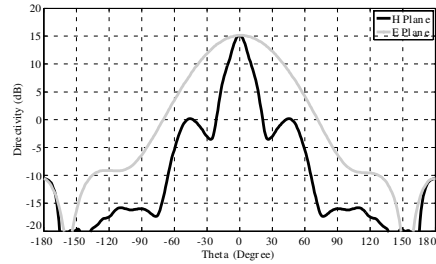
Figure 8. Radiation patterns at 5.29 GHz.

Figure 8 represents the radiation pattern in the vertical (H) and horizontal (E) planes of the antenna at 5.29 GHz.

The antenna is directive in the H plane and sectoral in the E plane (60°). The maximum directivity reaches 15.2 dB.

The design of an antenna working in horizontal polarization having been investigated, the vertically polarized antenna will now be studied.
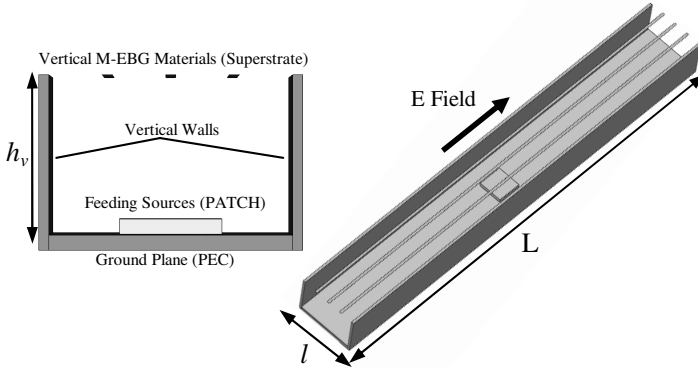
4. VERTICALLY POLARIZED SECTORAL M-EBG ANTENNA

The study is completely identical to the horizontally polarized antenna. The only difference is the calculation of the cavity height (5) [6, 13].

$$h_v = \frac{1}{2} \frac{c\left(\frac{1}{2} + \frac{\varphi_{M-EBG}}{2\pi}\right)}{\sqrt{f^2 - \frac{c^2}{4l^2}\left(\frac{\varphi_{Walls}}{\pi}\right)^2}} \tag{5}$$

With l the antenna width, $\varphi_{M-EBG} = 151°$, $\varphi_{Walls} = 180°$ at $5.3\,\text{GHz}$ correspond to the reflection phase of the walls defining the cavity.

This new antenna uses only a one-dimensional structure in TM polarization; the feed port and the metallic rods must be in a vertical distribution (Fig. 9).

Figure 9. Top and 3D view of the vertically polarized sectoral M-EBG antenna.

The vertical M-EBG layer is composed of 3 metallic rods of $375 \times 2\,\text{mm}^2$ and $12.5\,\text{mm}$ periodicity.

The simulated ground plane has the same size as the structure, i.e., $L = 375\,\text{mm} \times l = 52\,\text{mm}$.

The simulated performances yielded by the antenna in term of directivity and radiation pattern are displayed on Fig. 10 and Fig. 11.

The antenna performance obtained is correct in terms of given specifications. The angular aperture in the H Plane, reaches the prescribed value of $63°$. Only the operating frequency has a slight shift, since the maximum directivity is obtained at $5.4\,\text{GHz}$. The directivity reaches $15.5\,\text{dB}$ at the resonant frequency ($5.4\,\text{GHz}$).
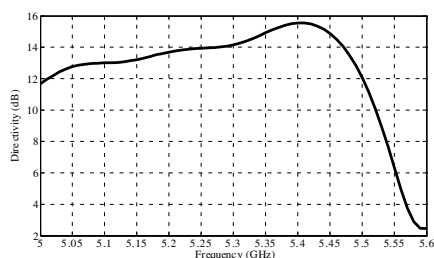
Combining horizontal and vertical structures, it is possible to create dual polarized M-EBG as it will be shown next.
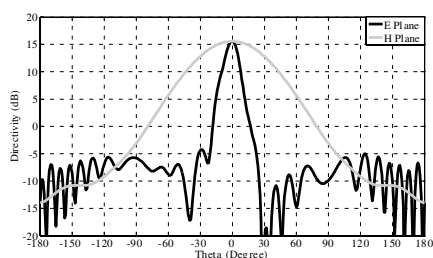
5. DUAL POLARIZED SECTORAL M-EBG ANTENNA

The concept can be summarized into the following two points:

1. The design of the upper M-EBG structure than having characteristics to achieve the desired gain-bandwidth for each polarization.
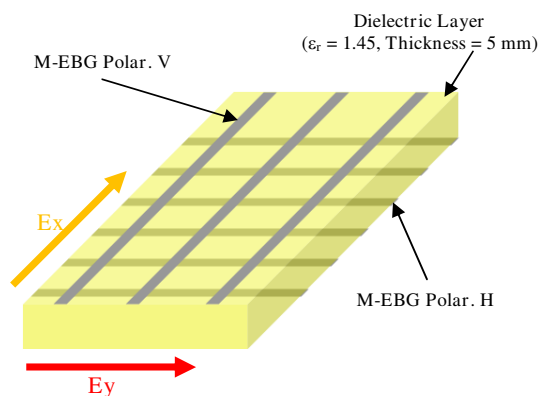
Figure 10. Directivity evolution versus frequency.

Figure 11. Radiation patterns at 5.4 GHz.

Figure 12. Geometry of the upper M-EBG structure.

2. The choice of a suitable feed source in the cavity which is capable of providing dual linear polarization.

5.1. Upper M-EBG Structure

A M-EBG structure is a polarizing filter because its response depends on the polarization of the incident wave. Stop and pass bands appear only when the electric field are parallel to metallic rods (TM polarization). Our M-EBG structure is composed of a sequence of metallic rods in order to reduce the antenna cost (Fig. 12).

The two M-EBG materials are working on orthogonal polarizations; they are thus transparent for each other. Since a single layer M-EBG superstrate in horizontal distribution (M-EBG Polar. H) assure the horizontal polarization, we stack another M-EBG layer in vertical distribution (M-EBG Polar. V) above the existing one, and adjust the distance between them in order to allow the vertical polarization

(Fig. 12). The dimensions for the dual polarization case are the same as ones for vertically or horizontally polarized antennas.

The two-layered M-EBG structures formed by metallic rods are printed on a dielectric whose thickness is 5 mm and the dielectric constant is 1.45.

5.2. Excitation Source

The dual polarized antenna is excited by a single patch, which is fed by two coaxial probes for controlling and switching between polarizations (Fig. 13). The patch dimensions are 20.5 mm × 20.5 mm, and it is printed on a 3 mm thickness dielectric substrate ($\varepsilon_r = 1.45$).

It is necessary to present the different possible polarizations of a patch with two feed probes (Table 1).
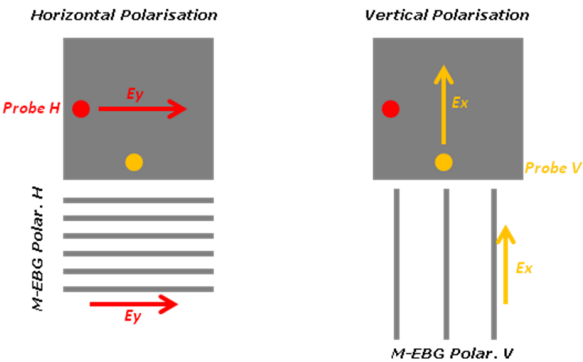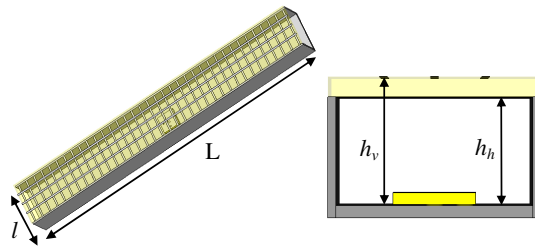
Figure 13. A patch antenna with two feed probes.

Table 1. Various configurations of a patch fed by two probes.

Probe H		Probe V		Polarization	
Amplitude	Phase	Amplitude	Phase		
1	X	0	X		Horizontal
0	X	1	X		Vertical
1	X	1	X+90°		Circular

Figure 14. Top and three-dimensional (3D) view of the Dual Polarized sectoral M-EBG antenna.

5.3. Antenna Geometry and Dimensions

We describe a dual polarized sectoral antenna design for WIMAX application [5.15–5.35] GHz with 15 dB directivity and a half power beamwidth of 60° in the horizontal plane.

The basic configuration of the proposed antenna is illustrated in Fig. 14. The Dual Polarized M-EBG antenna is composed of three principal parts (Fig. 14):

1. The ground plane where the feeding system (1 patch) is located.
2. The two-layered M-EBG structures as a superstrate made by periodic metallic elements.
3. The vertical walls to ensure the sectoral functionality of the antenna.

The first height is h_h between the M-EBG Polar. H and the ground plane, the second height is h_v between the ground plane and the M-EBG Polar. V. The two heights h_h and h_v are chosen to be 26.5 mm and 31.5 mm respectively in order to adjust the quality factor at each polarization and to utilize the resonant frequency around 5.3 GHz.

The simulated ground plane has the same size as the structure, i.e., $L = 375\,\text{mm} \times l = 52\,\text{mm}$.

6. EXPERIMENTAL VALIDATION

6.1. Fabricated Antenna

In order to validate the concept of the dual polarization antenna, a real structure based on the previous concept has been build.
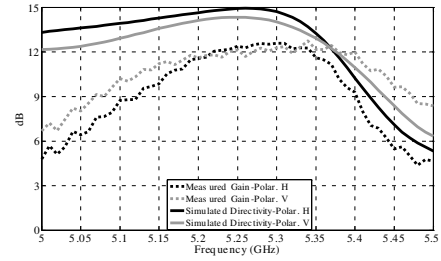
To facilitate the realization, both the M-EBG Polar. V and the M-EBG Polar. H have been positioned on the same printed circuit board made of dielectric layer ($\varepsilon_r = 1.45$) with 5 mm thick (Fig. 15).

Figure 15. Photographs of the dual polarized sectoral M-EBG antenna prototype.
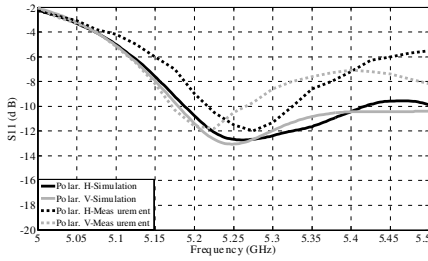
Figure 16. Return losses.

**Figure 17.** Simulated directivity and measured gain over frequency band.

A patch antenna is used to excite the resonant cavity (Fig. 15), it's printed on a foam plate ($\varepsilon_r = 1.45$, thick = 3 mm), fed by two SMA connectors and located on the ground plane.

The antenna structure was simulated with CST Microwave Studio, a FIT (Finite Integration Technique) based software. Measurements have been carried out with a HP-Agilent network analyzer and in an anechoic chamber belonging to XLIM for the radiation pattern, directivity and gain of the antenna.

6.2. Return Losses

Simulated and measured return losses are compared at each feed probes for the proposed dual polarization antenna (Fig. 16).

As shown in Fig. 16, return losses are less than −8 dB over the frequency range [5.15–5.35] GHz. That is, the antenna is well matched. However, the measured bandwidth is smaller than the simulated one. This reduction can be due to the dimension tolerances of the antenna.
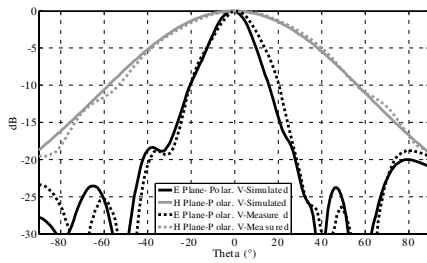
Figure 18. Measured and simulated E Plane, H Plane radiation patterns at 5.25 GHz for vertical polarization.
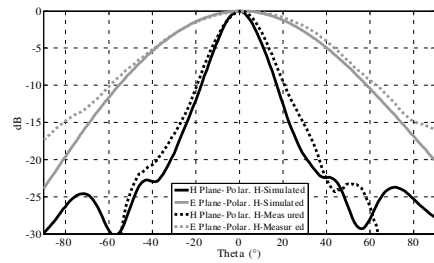
Figure 19. Measured and simulated E Plane, H Plane radiation patterns at 5.25 GHz for horizontal polarization.

6.3. Realized Gain

The maximum measured realized gain for each polarization is around 13 dB at 5.3 GHz, while the maximum simulated directivity is 14.5 dBi at 5.27 GHz (Fig. 17). This difference of values is due to different losses (dielectric and metallic losses, losses of coaxial cables which have been used during the measurement session, insertion losses and measurement equipment tolerances). Over the design bandwidth of 5.15 to 5.35 GHz, the variation in measured realized gain is within 2 dB of the maximum value.

6.4. Radiation Patterns

Figures 18 and 19 show the measured radiation patterns for each polarization in E and H planes, respectively, at 5.25 GHz, where we notice a very good agreement between the simulation and measurements. These results illustrate well the sectoral properties of the antenna over the band. In the vertical plane the radiation is directive with low side lobes, in the horizontal plane these figures present an interesting sectoral pattern of 60°.

The design of an antenna working in 0°/90° polarization having been investigated, the circularly polarized antenna will now be studied.

7. CIRCULARLY POLARIZED SECTORAL M-EBG ANTENNA

The 0°/90° dual polarized antenna study led to obtain equal vertical and horizontal components. This characteristic is a first step towards designing a circularly polarized antenna.

In order to obtain an antenna providing circular polarization, two criteria are required:

- Both vertical and horizontal components must have the same magnitude.
- The phase difference between horizontal and vertical components is 90°.

It therefore lacks to satisfy the phase difference condition between the two field components (E_x, E_y) to prove the feasibility of the circularly polarized antenna. The upper M-EBG structure did not differ from that used for 0°/90° polarization (Fig. 12). It must produce both polarizations simultaneously. Design dimensions are always the same as the 0°/90° dual polarized antenna. We just need to feed both horizontal and vertical polarization at the same time and achieve the proper 90° phase difference $\Delta\varphi$.

7.1. The Problem

By exciting the two feed probes H and V simultaneous with the same magnitude and a 90° phase shift, we generate a circular polarization of the patch (Table 1). By doing this, we have observed that the two orthogonal electric fields E_x and E_y of the M-EBG antenna undergo attenuation and a phase difference of $\Delta\varphi \approx 65° \neq 90°$ due to the asymmetric structure, vertical metallic walls and the upper M-EBG structure behavior.

First, it is necessary to show the polarization quality in terms of the ratio E_x/E_y (Fig. 20) and the phase difference $\Delta\varphi$ between E_x and E_y (Fig. 21).
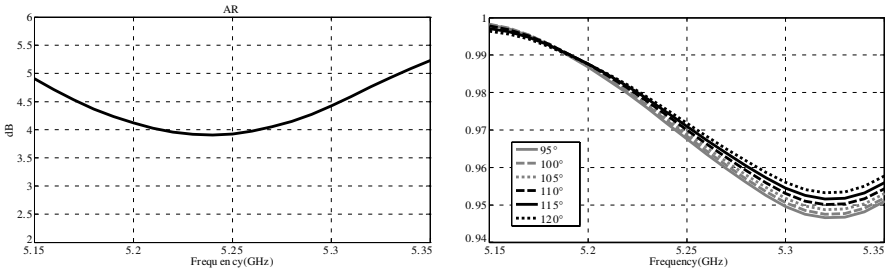
By observing the two previous curves in the frequency band [5.15–5.35] GHz, it is possible to see that the ratio E_x/E_y is approximately equal to unity and the phase difference is equal to $\Delta\varphi \approx 65°$.
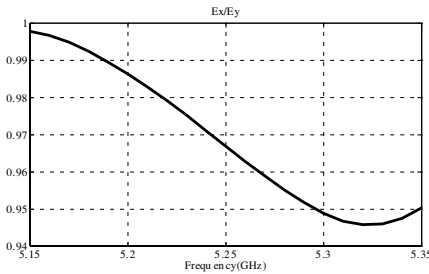
Figure 20. Ratio of field components E_x/E_y.
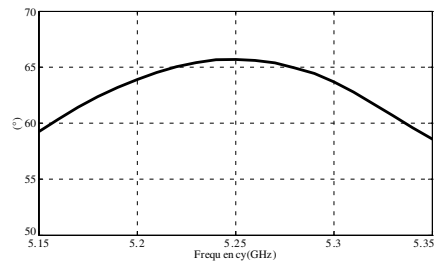
Figure 21. Phase difference $\Delta\varphi$ between E_x and E_y components.

Figure 22. Axial Ratio versus frequency.

Figure 23. Ratio of field components E_x/E_y for each case of phase shifts.

Table 2. Phase shift between H and V probes of the excitation patch.

Probe H		Probe V	
Amplitude	Phase	Amplitude	Phase
1	X	1	X + 95°
1	X	1	X + 100°
1	X	1	X + 105°
1	X	1	X + 110°
1	X	1	X + 115°
1	X	1	X + 120°

Figure 22 shows the Axial Ratio AR of the M-EBG antenna when we excite the patch by the third configuration shown in Table 1.

Over the whole frequency band, the AR is very poor and varies between 4 and 5 dB. It is shown that, with a 90° phase shift between the two feed probes H and V, it is unthinkable to generate circular polarization. Both E_x and E_y fields had a phase difference of $\Delta\varphi \approx 65°$ between them even though they have almost the same magnitude.

To correct the phase defect in order to obtain a phase difference of $\Delta\varphi \approx 90°$ between components, it is necessary to induce a phase shift greater than 90° between the H and V probes to improve the circular polarization quality by decreasing the 3 dB AR.
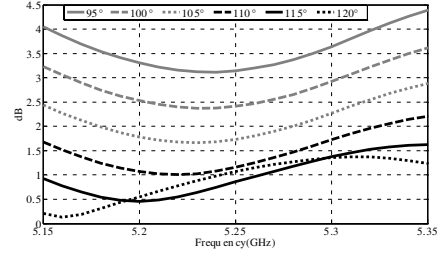
7.2. Influence of the Phase Shift between H and V Feed Probes

Studied phase shift values between feed probes are presented in Table 2.

It is essential to understand how the phase shift between feed probes influences the performance of the circularly polarized antenna.
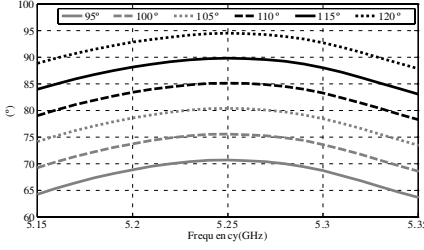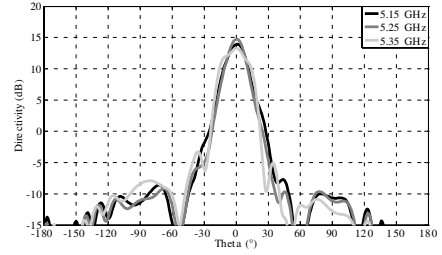
Figure 24. Phase difference $\Delta\varphi$ between E_x and E_y components for each case of phase shifts.

Figure 25. Axial ratio versus frequency for each case of phase shifts.
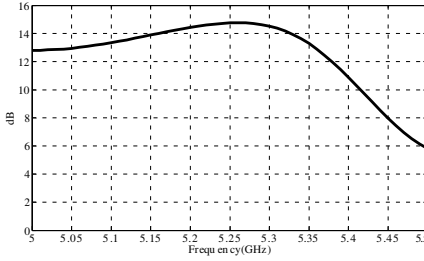
Figure 26. Directivity evolution over frequency band.

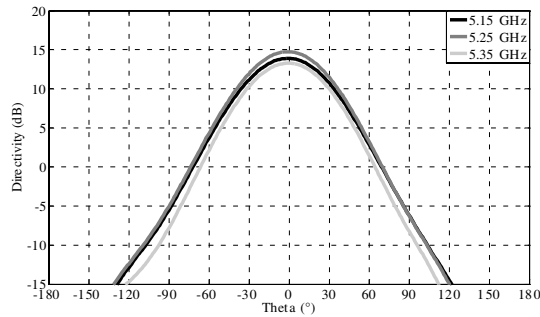**Figure 27.** Radiation patterns in the vertical plane.

To do this, we will present the ratio E_x/E_y (Fig. 23) and the phase difference $\Delta\varphi$ between E_x and E_y components (Fig. 24) for each case listed in Table 2.

According to our expectations, by increasing the phase shift between feed probes, the phase difference $\Delta\varphi$ between E_x and E_y components approaches $90°$. Best results are obtained with phase shift of $115°$ between probes. With this phase shift, the phase difference between components is increased from $\Delta\varphi \approx 65°$ to $\Delta\varphi \approx 90°$ over the frequency band [5.15–5.35] GHz. This phase shift between probes corrects the phase difference $\Delta\varphi$ without perturbing magnitude fields.

It is necessary to see if phase shifts bring improvements in the AR over the frequency band. Fig. 25 shows AR versus frequency for each case of phase shifts listed in Table 2.

We can therefore say that the $115°$ phase shift between the feed probes H and V is useful for providing a pure circular polarization with a ratio E_x/E_y tending to 1 and a phase difference of $\Delta\varphi \approx 90°$. The AR varies between 0.45 and 1.5 dB over the operating band [5.15–5.35] GHz.

Figure 28. Radiation patterns in the horizontal plane.

7.3. Antenna Performances

The results are presented for the circularly polarized antenna with a 115° phase shift between the two feed probes H and V.

The performance yielded by the antenna in term of directivity is displayed on Fig. 26. A maximum directivity of 14.7 dB has been obtained, which is consistent with the intended values.

Radiation patterns at 5.15, 5.25 and 5.35 GHz in the vertical and horizontal planes are presented in Fig. 27 and Fig. 28 respectively. These frequencies were chosen to correspond to the lower, center, and upper operate frequencies of the antenna.

The radiation angle in the horizontal plane is correct, being higher than 60° on the whole frequency band. The antenna is directive in the vertical plane. The patterns have low side lobes, so we can estimate that the structure is well dimensioned.

8. CONCLUSION

A novel multipolarized sectoral antenna has been described, fabricated and measured at [5.15–5.35] GHz. M-EBG structures and a patch fed by two probes were combined to realize multipolarisation capability. The simulated and measured characteristics meet the specified requirements between 5.15 GHz and 5.35 GHz. This paper shows the possibility for M-EBG antennas to radiate in vertical, horizontal, 0°/90° and circular polarizations with a sectoral pattern in azimuth.

A new technique of improving the quality of the circularly polarized antenna is studied. The effect of the phase shift between feed probes has enhanced the polarization purity with 1.5 dB Axial Ratio over the frequency band.

The designed antenna showed desirable performances in terms of

directivity and beamwidth. This antenna is an excellent candidate for several applications owing to its multipolarization properties. The proposed structure dispenses with the need for complex feeding mechanisms of patch array antennas.

REFERENCES

1. Lindmark, B. and M. Nilsson, "On the available diversity gain from different dual-polarized antennas," *IEEE J. Select. Areas Commun.*, Vol. 19, No. 2, 287–294, Feb. 2001.

2. Carver, K. R. and J. W. Mink, "Microstrip antenna technology," *IEEE Transactions on Antennas and Propagation*, Vol. 29, No. 1, Jan. 1981

3. Hall, P. S., "Review of techniques for dual and circularly polarized microstrip antennas," *Microstrip Antennas, The Analysis and Design of Microstrip Antennasand Arrays*, D. M. Pozar and D. H. Schaubert (eds.), IEEE Press, New York, 1995.

4. Yun, W. S. and S. W. Kwon, "Wideband microstrip antennas for PCS/IMT-2000 services," *IEEE Symposium on Antennas and Propagation*, Vol. 3, 1398–1401, 2000.

5. Thevenot, M., C. Cheype, A. Reineix, and B. Jecko, "Directive photonic bandgap antennas," *IEEE Transaction on Microwave Theory and Techniques*, Vol. 47, No. 11, 2115–2122, Nov. 1999.

6. Cheype, C., C. Serier, M. Thevenot, T. Monediere, A. Reineix, and B. Jecko, "An electromagnetic bandgap resonator antenna," *IEEE Transactions on Antennas and Propagation*, Vol. 50, No. 9, 1285–1290, Sep. 2002.

7. Jackson, D. R. and N. G. Alexopoulos, "Gain enhancement methods for printed circuit antennas," *IEEE Transactions on Antennas and Propagation*, Vol. 33, No. 9, 976–987, Sep. 1985.

8. Qiu, M. and S. He, "High directivity patch antenna with both photonic bandgap substrate and photonic bangap cover," *Microw. Opt. Technol. Lett.*, Vol. 30, No. 1, 41–44, Jul. 2001.

9. Trentini, G. V., "Partially reflecting sheet arrays," *IEEE Transactions on Antennas and Propagation*, Vol. 4, No. 4, 666–671, Oct. 1956.

10. Palikaras, G. K., A. P. Feresidis, and J. C. Vardaxoglou, "Cylindrical electromagnetic bandgap structures for directive base station antennas," *IEEE Transactions on Antennas and Propagation*, Vol. 3, No. 1, 87–89, 2004.

11. Feresidis, A. P. and J. C. Vardaxoglou, "High gain planar antenna

using optimized partially reflective surfaces," *IEE Proc. Microw. Antennas Propag.*, Vol. 148, No. 6, 345–350, 2001.

12. Foroozesh, A. and L. Shafai, "Investigation into the effects of the patch-type FSS superstrate on the high-gain cavity resonance antenna design," *IEEE Transactions on Antennas and Propagation*, Vol. 58, No. 2, 258–270, Feb. 2010.

13. Hajj, M., H. Chreim, E. Rodes, E. Arnaud, D. Serhal, and B. Jecko, "Rectangular M-PRS structure for sectoral base station antenna with vertical polarization," *Microw. Opt. Technol. Lett.*, Vol. 52, No. 4, 990, 2010.

14. Sauleau, R., "Fabry perot resonators," *Encyclopedia of RF and Microwave Engineering*, 1381–1401, John Wiley and Sons, 2005.

15. Combes, P. F., *Micro-Ondes*, 228–237, Tome 2, Dunod, Paris, France, 1997.

16. Vardaxoglou, J. C., *Frequency Selective Surfaces: Analysis and Design*, Research Studies, Somerset, UK, 1997.